Reactivity of Phosphate Monoester Monoanions in Aqueous Solution. 2. A Theoretical Study of the Elusive Zwitterion Intermediates $RO^+(H)PO_3^{2-}$

Marc Bianciotto,[†] Jean-Claude Barthelat,[‡] and Alain Vigroux*,[†]

Laboratoire de Synthèse et Physico-Chimie de Molécules d'Intérêt Biologique (UMR 5068), and Laboratoire de Physique Quantique, IRSAMC (UMR 5626), Université Paul Sabatier, 118 Route de Narbonne, 31062 Toulouse Cedex 4, France

Received: April 23, 2002

In a previous theoretical study [*J. Am. Chem. Soc.*, in press], using a combination of DFT and continuum solvation (PCM) methods, the anionic zwitterion $CH_3O^+(H)PO_3^{2-}$ (**2**) has been identified as a key intermediate in the mechanism for the dissociative hydrolysis of the methyl phosphate anion $CH_3OPO_3H^-$ (**1**). To confirm this finding, DFT/B3LYP calculations in which a few solvent molecules are explicitly considered, are reported. Hydrogen-bonded complexes $\mathbf{2}\cdot(H_2O)_n$ ($n = 2-4$) have been fully optimized and characterized on their respective potential energy surfaces. We have shown that only two specifically solvating water molecules are sufficient to reproduce the PCM results previously obtained provided they occupy a critical bridging position between the methanol and metaphosphate fragments. Further, DFT-PCM geometry optimizations of $RO^+(H)PO_3^{2-}$ (R = phenyl and 2,4-dinitrophenyl) agree with predictions, based on the mechanistic picture proposed by Kirby and Varvoglis [*J. Am. Chem. Soc.* **1967**, *89*, 415] 35 years ago, according to which anionic zwitterions are assumed to exist as intermediates for the methyl and phenyl esters but not for the 2,4-dinitrophenyl ester. Moreover, biologically important counterions such as Mg^{2+} can also play a crucial role in stabilizing the zwitterionic structure $RO^+(H)PO_3^{2-}$ in the gas phase.

Introduction

In the first paper of this series,[1] we have provided the first theoretical evidence that supports the long-standing mechanistic hypothesis involving the zwitterionic species $CH_3O^+(H)PO_3^{2-}$ (**2**) as an intermediate during the dissociative hydrolysis reaction of the monoanion of methyl phosphate monoester (**1**). In agreement with much experimental information, our density functional theory (DFT) calculations performed with the implicit solvation model PCM[2] confirmed that the essential features of the monoanion reaction include (i) a preequilibrium proton transfer from the phosphate hydroxy ligand to the esterified oxygen (via at least one intervening water molecule) and (ii) subsequent P−O bond cleavage of the transient zwitterion intermediate **2** in the rate-determining step (Scheme 1). According to our results, the latter process may occur either through a stepwise $D_N + A_N$ dissociative mechanism involving the generation of solvated metaphosphate ion as an intermediate or through a concerted A_ND_N mechanism with a single metaphosphate-like transition state in which the nucleophile and the leaving group are both weakly coordinated to phosphorus.

Anionic zwitterions $RO^+(H)PO_3^{2-}$ (R = alkyl) were postulated as intermediates in the hydrolysis of phosphate monoester monoanions as early as 1962 by Jencks[3] who first proposed the mechanistic pathway shown in Scheme 1 as a possible route for hydrolysis. Since that time, indirect experimental evidence has accumulated in support of this path and of the intermediacy of $RO^+(H)PO_3^{2-}$ species,[4] thus making the mechanistic picture

SCHEME 1: Commonly Accepted Pathway for the Hydrolysis Reaction of Phosphate Monoester Monoanions (rds: Rate-Determining Step)

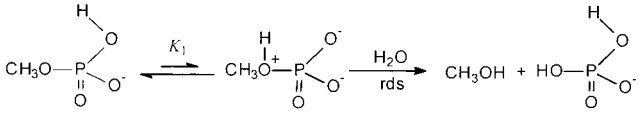

of Scheme 1 widely accepted by chemists.[5] However, the actual involvement of anionic zwitterions in the hydrolysis of the monoanions has not been demonstrated so far. Clearly, these dipolar species are probably too unstable to exist as isolable, or even observable, intermediates. Therefore, in the absence of any direct experiment that would provide unique evidence of their formation, quantum-mechanical calculations become a valuable alternative. Hence, we can ask important questions concerning (1) the reliability of implicit models of solvation (as, e.g., the PCM model used in our previous paper[1]) to describing properly the aqueous environment in which anionic zwitterions $RO^+(H)PO_3^{2-}$ are expected to be formed, (2) the effect of the nature of the leaving group ROH, and (3) the possible role played by biologically relevant counterions at stabilizing such species.

In the present study we will report results of DFT calculations aimed at determining whether **2** can be identified as an intermediate during the dissociative hydrolysis of **1** in the gas phase in the presence of only a few water molecules (water vapor), thus confirming or not our previously reported PCM results.[1] Specific solvation effects have, therefore, been tackled using the supermolecule approach in which the solvent molecules are considered explicitly. Thus, to determine the possible role played by the first solvation shell on the preequilibrium

* To whom correspondence should be addressed at the following: E-mail: vigroux@chimie.ups-tlse.fr. Fax: (+33)5-61-55-60-11.

[†] Laboratoire de Synthèse et Physico-Chimie de Molécules d'Intérêt Biologique.

[‡] Laboratoire de Physique Quantique.

10.1021/jp021036b CCC: $22.00
Published on Web 06/11/2002

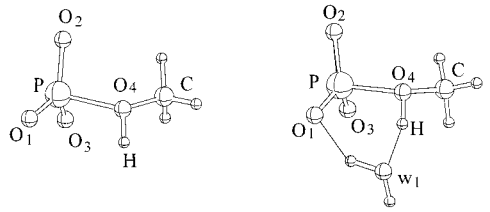

Figure 1. B3LYP-PCM optimized geometries of the zwitterionic species **2** (left) and **2**·H_2O (right) in aqueous solution.

formation of **2**, we have performed geometry optimizations, without a surrounding continuum, on clusters consisting of anionic zwitterion **2** and up to four water molecules, **2**·$(H_2O)_n$ ($n = 0-4$). For the sake of comparison with the PCM results, all structures of interest were optimized at the same level of theory, this includes the corresponding reactant and transition state structures **1**·$(H_2O)_n$ and TS(**6c**)·$(H_2O)_{n-1}$, respectively.

We will also focus on the PCM structures $RO^+(H)PO_3^{2-}$ as a function of R (R = H, methyl, phenyl, and 2,4-dinitrophenyl) and will discuss briefly the bonding characteristics of the P−O bond between the bridging methyl oxygen and phosphorus in $CH_3O^+(H)PO_3^{2-}$ on the basis of natural bond orbital (NBO)[6] analysis and molecular orbitals. Finally, we hope that the results of the present study will have instructive implications in stimulating and guiding new experimental and theoretical studies on the subject.

Theoretical Methods

All calculations were performed with the Gaussian 98 set of programs[7] following the same procedure as in the previous related paper[1] (pseudopotentials and double-ζ plus polarization valence basis sets[8] with s and p diffuse functions added to oxygen atoms; see ref 1). The nature of the six-centered transition states TS(**6c**)·$(H_2O)_{n-1}$ involved in the prototropic rearrangement **1**·$(H_2O)_n \rightarrow$ **2**·$(H_2O)_n$ ($n = 2-4$) was verified by a single imaginary frequency (Table 5) and an intrinsic reaction coordinate (IRC) calculation leading to the expected ground state and product.

Results and Discussion

Zwitterionic Structures 2·$(H_2O)_n$ ($n = 0-4$). In our previous theoretical study,[1] evidence was provided that anionic zwitterions $RO^+(H)PO_3^{2-}$ (R = H, CH_3) could be located, with the PCM solvation model, as stable intermediates (i.e., minima) along the reaction path involved in the dissociative hydrolysis of the methyl phosphate anion $CH_3OPO_3H^-$ (**1**). Thus, making use of this model of solvation, we were able to characterize the naked zwitterionic form **2** of methyl phosphate **1** along with its corresponding hydrated species **2**·H_2O, in which a complexing water molecule is hydrogen bonded to **2** via a six-membered-ring structure. The fully optimized PCM structures of **2** and **2**·H_2O are shown in Figure 1. Selected geometrical parameters for **2** and **2**·H_2O are summarized in Table 1. It is clear from Figure 1 and Table 1 that the $CH_3O^+(H)PO_3^{2-}$ unit does not change dramatically in the presence of one H_2O molecule. There is, however, two significant structural changes due to the presence of the water molecule: (i) the decrease (ca. 5.1%) of the bond distance P−O_4 from 2.029 to 1.926 Å and (ii) the increase (ca. 4.7%) of the bond distance O_4−H from 0.981 to 1.027 Å. The first change suggests that in the ion−molecule complex **2**·H_2O the bridging position of the H_2O molecule (Figure 1) prevents the metaphosphate and methanol parts to move further away from each other, thus stabilizing the zwitterionic form **2** relative to its dissociation into methanol and metaphosphate. The second change corroborates with the calculated O_{W1}- - -H distance of 1.575 Å (Table 1). Such a value is indicative of the presence of a rather strong hydrogen bond between O_{W1} and H (Figure 1), which should render the O_4−H bond in **2**·H_2O weaker than in the naked species **2**.

TABLE 1: Selected Geometrical Parameters for Fully Optimized 2 and 2·$(H_2O)_n$ Species Including One Bridging Water Molecule between the Metaphosphate and Methanol Fragments, with Solvation Correction (PCM), and in the Gas Phase (Gas)[a]

	PCM[b,c]		gas[d]		
	$n = 0$	$n = 1$	$n = 2$	$n = 3$	$n = 4$
P−O_1	1.512	1.527	1.526	1.524	1.524
P−O_2	1.512	1.510	1.496	1.503	1.510
P−O_3	1.512	1.514	1.520	1.523	1.521
P−O_4	2.029	1.926	2.288	2.089	2.025
C−O_4	1.457	1.456	1.428	1.436	1.444
O_4−H	0.981	1.027	0.996	1.014	1.021
O_{W1}−H		1.575	1.764	1.666	1.628
O_1−H_{W1}		1.715	1.756	1.826	1.842
O_{W2}−H_{W1}			2.162	1.872	1.850
O_3−H_{W2}			1.820	1.621	1.656
O_1−H_{W3}				2.138	2.091
O_2−H_{W3}				2.080	2.104
O_2−H_{W4}				−	2.099
O_3−H_{W4}				−	2.146
P−O_4−H	110.4	105.8	100.3	102.0	101.6
O_4−H−O_{W1}		159.4	157.1	158.1	159.7
H−O_{W1}−H_{W1}		86.5	79.8	84.1	86.2
O_{W1}−H_{W1}−O_1		148.3	156.0	151.0	148.7
H_{W1}−O_1−P		109.9	113.8	108.5	107.0
O_1−P−O_4		95.8	91.2	93.6	96.0

[a] All distances are in angstroms and angles in degrees. [b] The conventional set of Pauling radii and a dielectric constant of 78.39 were used for calculations; see ref 1 for details. [c] The optimized structures are depicted in Figure 1. [d] The optimized structures are depicted in Figure 2.

It is of interest to note that the calculated distances O_4- - -H in **2**·$(H_2O)_n$ structures (Table 1) clearly indicate that the proton is attached to the bridging methyl oxygen O_4. Thus, as expected, the P−O_4 bond is quite elongated in **2** (+0.385 Å, ca. +23%) and **2**·H_2O (+0.281 Å, ca. +17%) relative to the reactant values[1] of 1.644 (**1**) and 1.645 Å (**1**·H_2O), respectively. In contrast, the C−O_4 bond is not significantly elongated in **2** and **2**·H_2O (ca. 1% increase) relative to the values reported[1] for the isomeric structures **1** and **1**·H_2O.

Our DFT calculations on **2** and **2**·H_2O indicate that the tautomeric form **2** does not exist in the gas phase as a stable structure unless two or more water molecules are present. While it is well-known that organic zwitterions commonly occur in solution, the stabilizing effect of solvent on these dipolar species, either as a dielectric continuum (bulk effect) or as an ensemble of individual interacting molecules, is much less established. In our previous study,[1] we found that the tautomeric forms $RO^+(H)PO_3^{2-}$ and $RO^+(H)PO_3^{2-}$·H_2O are intrinsically unstable in the gas phase. Each species was found to collapse into its corresponding molecular complex ROH·PO_3^- or ROH·PO_3^-·H_2O. However, the present calculations indicate that it is possible to locate the tautomeric form $CH_3O^+(H)PO_3^{2-}$ in the gas phase with as few as two water molecules. The fully optimized structure **2**·$(H_2O)_2$ so obtained is shown in Figure 2, and its selected geometrical parameters are listed in Table 1.

We anticipated the bridging water molecule of **2**·$(H_2O)_2$ (W_1 in Figure 2) to play a critical role in maintaining the zwitterionic character of **2** and found that, indeed, **2**·$(H_2O)_2$ could not exist in the gas phase without involving a bridging water molecule between methanol and metaphosphate fragments. In contrast, a

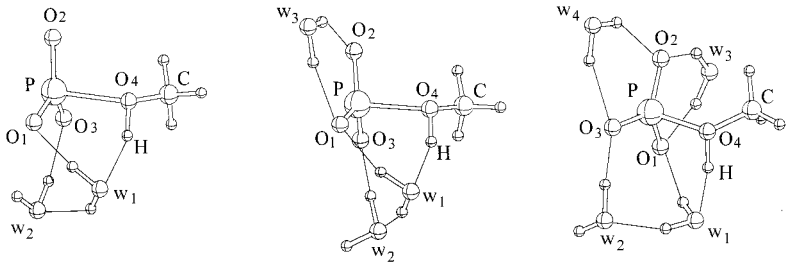

Figure 2. B3LYP optimized structures for the hydrated zwitterions **2**·$(H_2O)_n$ ($n = 2-4$) in the gas phase.

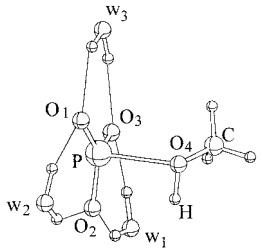

Figure 3. B3LYP optimized structure for a trihydrated zwitterionic species with no bridging water molecule between methanol and metaphosphate fragments.

TABLE 2: P−O_4 Distance[a] of Fully Optimized 2·$(H_2O)_n$ Species in the Gas Phase[b]

	no bridging H_2O[a]		one bridging H_2O[a]			
	$n = 0-2$	$n = 3$	$n = 0-1$	$n = 2$	$n = 3$	$n = 4$
P−O_4 (Å)	dissoc	2.34	dissoc	2.29	2.09	2.03

[a] Between metaphosphate and methanol parts. [b] The optimized structures are depicted in Figures 2 and 3.

trihydrated zwitterionic species, depicted in Figure 3, could be located without involving a bridging water molecule between the two fragments. The stabilizing influence of the bridging W_1 molecule of **2**·$(H_2O)_2$ becomes evident when we compare (Table 2) the P−O_4 bond length of this structure (2.29 Å) with that of the trihydrated structure shown in Figure 3 (2.34 Å).

The effects of both the number and the position of water molecules on the stability of **2** (relative to its dissociation into methanol and metaphosphate) are summarized in Table 2. The fully optimized **2**·$(H_2O)_n$ species ($n = 2-4$) including one bridging H_2O molecule are presented in Figure 2. The corresponding selected geometrical parameters are listed in Table 1. It is clear from Table 2 that the greatest effect to favor the dipolar structure **2** is by including a water molecule that bridges the methanol and metaphosphate moieties by acting both as a hydrogen bond acceptor and donor. The presence of the third H_2O molecule (corresponding to W_3 in the **2**·$(H_2O)_3$ structure shown in Figure 2), which is hydrogen bonded to the phosphate oxygens O_1 and O_2, results in a further significant decrease of the P−O_4 bond distance from 2.29 to 2.09 Å. As can be seen in Tables 1 and 2, no major structural changes for the

TABLE 3: Selected Distances for Fully Optimized 1·$(H_2O)_n$ Reactant Species in the Gas Phase ($n = 2-4$)[a]

	gas[b]		
1·$(H_2O)_n$	$n = 2$	$n = 3$	$n = 4$
P−O_1	1.525	1.533	1.519
P−O_2	1.505	1.501	1.509
P−O_3	1.649	1.623	1.638
P−O_4	1.655	1.680	1.660
C−O_4	1.427	1.432	1.436
O_3−H	0.983	0.992	0.992
O_{W1}−H	2.046	1.895	1.867
O_1−H_{W1}	1.657	(3.138)	(3.083)
O_1−H_{W2}	2.139	2.109	2.147
O_2−H_{W2}	2.056	2.050	2.115
O_1−H_{W3}		1.594	1.612
O_{W3}−H_{W1}		1.815	1.786
O_4−H_{W1}		2.176	2.434
O_2−H_{W4}			1.854
O_3−H_{W4}			2.574

[a] All distances are in angstroms. [b] The corresponding optimized structures are depicted in Figure 4.

$CH_3O^+(H)PO_3^{2-}$ unit occur when more than three water molecules are brought into the system. The decrease of the P−O_4 bond length due to the fourth water is much smaller in magnitude than the decrease due to the third water (0.06 vs 0.2 Å, respectively). Finally, it is interesting to note that when the zwitterionic structure **2** is hydrated by four H_2O molecules (**2**·$(H_2O)_4$, Figure 2), then its optimized structure in the gas phase strongly resembles that obtained for the naked species with the PCM model (**2**, Figure 1).

Reactants 1·$(H_2O)_n$ and Water-Assisted Transition Structures TS(6c)·$(H_2O)_{n-1}$ ($n = 2-4$). To determine the energetics associated with the prototropic rearrangement K_1 (Scheme 1) in the gas phase, we performed, at the same level of theory, geometry optimizations of methyl phosphate anion in the presence of two, three, and four water molecules. The corresponding reactant structures 1·$(H_2O)_n$ are depicted in Figure 4 and a set of selected distances is provided in Table 3. As expected, the solvating water molecules form bridges between the H−O and O−P bonds of the phosphate anion, giving six- (or eight-) membered ring structures. Comparing with the gas-phase geometry of free $CH_3OPO_3H^-$,[1] it can be seen that the

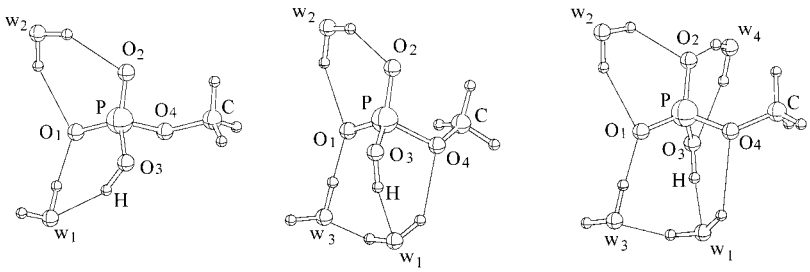

Figure 4. B3LYP optimized structures for the reactant species 1·$(H_2O)_n$ ($n = 2-4$) in the gas phase.

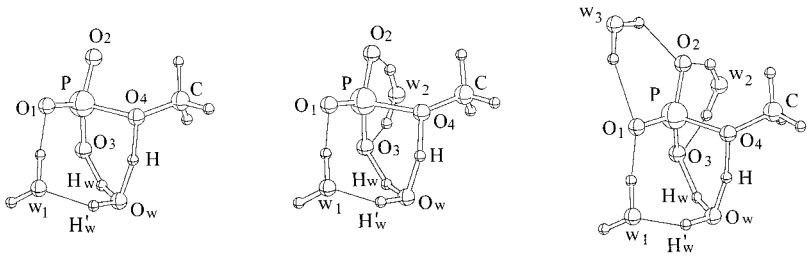

Figure 5. B3LYP optimized structures of gas-phase transition states TS(**6c**)·$(H_2O)_{n-1}$ ($n = 2-4$) for the proton-transfer process **1**·$(H_2O)_n \rightarrow$ **2**·$(H_2O)_n$.

TABLE 4: Selected Geometrical Parameters for Fully Optimized Six-Centered Water-Assisted Transition States TS(6c)·$(H_2O)_{n-1}$ in the Gas Phase ($n = 2-4$)[a]

	gas[b]		
TS(**6c**)·$(H_2O)_{n-1}$	$n = 2$	$n = 3$	$n = 4$
$P-O_1$	1.525	1.523	1.529
$P-O_2$	1.500	1.506	1.511
$P-O_3$	1.559	1.562	1.551
$P-O_4$	1.910	1.869	1.846
$C-O_4$	1.433	1.438	1.442
O_4-H	1.198	1.226	1.235
O_W-H	1.249	1.220	1.211
O_W-H_W	1.114	1.080	1.059
O_3-H_W	1.379	1.452	1.512
$O_{W1}-H'_W$	1.855	1.774	1.736
O_1-H_{W1}	1.595	1.586	1.600
O_2-H_{W2}		2.021	2.077
O_3-H_{W2}		2.092	2.085
O_1-H_{W3}			2.103
O_2-H_{W3}			2.116
$P-O_4-H$	99.1	99.6	99.9
O_4-H-O_W	160.1	159.7	159.6
$H-O_W-H_W$	85.4	87.1	88.3
$O_W-H_W-O_3$	158.7	155.6	153.0
H_W-O_3-P	105.8	105.0	104.7
O_3-P-O_4	95.8	96.7	97.7

[a] All distances are in angstroms and angles in degrees. [b] The corresponding optimized structures are depicted in Figure 5.

O_3-H and $C-O_4$ bonds are larger by about 0.02 Å while the other bonds remain essentially unchanged.

The geometries of the water-assisted transition states for the proton-transfer process **1** → **2** were also optimized in the presence of explicit water molecules. The corresponding structures TS(**6c**)·$(H_2O)_{n-1}$ are shown in Figure 5, and selected geometrical parameters are listed in Table 4. One H_2O molecule noted $H_WO_WH'_W$ (W) plays a central role in assisting proton transfer (via a six-membered ring structure) between the metaphosphate and methanol fragments. The critical position of W is maintained by a second water molecule (W_1 in Figure 5) which hydrogen bonds to both the phosphoryl oxygen O_1 and H'_W. The remaining water molecules (referred to as W_2 and W_3 in Figure 5) interact directly with the phosphoryl oxygens. As can be seen in Table 4 ($n = 3$, 4), these additional H_2O molecules do not substantially alter the geometry of the six-centered transition state TS(**6c**)·H_2O.

Energetics. Table 5 lists the calculated free energies in aqueous solution (with respect to the solvated reactants **1**·$(H_2O)_n$) for the stationary points involved in the preequilibrium formation of anionic zwitterions **2**·$(H_2O)_n$ (K_1, Scheme 1) as a function of the number of explicit water molecules. For each supermolecule investigated ($n = 2-4$), the effect of solvation was taken into account through single-point energy calculations at the PCM level of theory. Our results indicate that the presence of a continuum does not greatly modify the relative gas-phase free energy values. As can be seen in Table 5, the computed

TABLE 5: Relative B3LYP Gas-Phase Energy (ΔE), Zero-Point Vibrational Energy (ΔZPE), Enthalpy (ΔH), Entropy Contribution ($T\Delta S$), Gas-Phase Free Energy (ΔG_{gas}), Solvent Contribution to Free Energy (ΔW_0), Free Energy in Aqueous Solution (ΔG_{aq}), and Transition Frequencies of TSs (ν_{gas}) for the Stationary Points Involved in the Proton Transfer Process Occurring during the First Stage of the Dissociative Hydrolysis of $CH_3OPO_3H^-$ in the Gas Phase with Two, Three, and Four Water Molecules at 298 K[a]

	gas							
structure[b]	ΔE	ΔZPE	ΔH	$T\Delta S$	ΔG_{gas}	ΔW_0[c]	ΔG_{aq}[d]	ν_{gas}
1·$(H_2O)_2$	0.0	0.0	0.0	0.0	0.0	0.0	0.0	
TS(6c)· H_2O	23.5	−2.6	19.7	−3.7	23.4	−1.0	22.4	988i
2·$(H_2O)_2$	21.3	0.4	21.9	−0.1	22.0	−0.6	21.4	
1·$(H_2O)_3$	0.0	0.0	0.0	0.0	0.0	0.0	0.0	
TS(6c)·$(H_2O)_2$	21.7	−2.6	18.1	−2.6	20.7	−0.5	20.2	845i
2·$(H_2O)_3$	18.6	0.1	18.7	−0.1	18.8	0.8	19.6	
1·$(H_2O)_4$	0.0	0.0	0.0	0.0	0.0	0.0	0.0	
TS(6c)·$(H_2O)_3$	21.0	−2.1	17.7	−3.2	20.9	1.1	22.0	748i
2·$(H_2O)_4$	18.1	0.4	18.4	−1.1	19.5	0.9	20.4	

[a] Units are kcal/mol for energies and cm^{-1} for imaginary frequencies. [b] The optimized structures are depicted in Figures 2, 4, and 5. [c] Relative solvation free energy computed with the polarizable continuum model PCM by using UATM radii and a dielectric constant of 78.39. [d] $\Delta G_{aq} = \Delta G_{gas} + \Delta W_0$.

PCM solvation free energies ΔW_0 are small (i.e., <5% of ΔG_{gas}) so that free energies in solution, ΔG_{aq}, are close to their corresponding values in the gas phase. On the whole, it seems that the role of the surroundings (bulk solvent effect) is less decisive than the specific action of a catalytic cluster.

On the other hand, the values of ΔG_{aq} do not change significantly with an increase of the cluster size. As previously noted by Hu and Brinck in a similar theoretical approach,[9] this can be attributed to the fact that the added water molecules (W_2 and W_3 in Figure 5) do not play an active, direct or indirect, catalytic role in the transition state. Surprisingly, the presence of only two *active* water molecules in a position appropriate to bridge the metaphosphate and methanol parts (as W_1 and W_2 in Figure 2, or W and W_1 in Figure 5), is sufficient to give values of ΔG_{gas} and ΔG_{aq} in good agreement with the ΔG_{PCM} free energy values directly obtained from PCM geometry optimizations and frequency calculations on the reactant species **1**·H_2O (denoted **1a** in the previous paper;[1] compare the values of ΔG_{gas} and ΔG_{aq} for $n = 2$ with the values of ΔG_{PCM} reported for **1a**, TS**1a**−**2a** and **2a** in Table 3 of ref 1). Since the calculated free energies in the gas and aqueous phases vary only slightly with *n*, a reasonably good agreement is obtained for all the catalytic cluster investigated. For example, the free energy difference in aqueous solution is calculated to be $\Delta G_{aq} = 20.4$ kcal/mol between **1**·$(H_2O)_4$ and **2**·$(H_2O)_4$, and $\Delta G_{PCM} = 20.8$ kcal/mol between **1**·H_2O (**1a**) and **2**·H_2O (**2a**). It can also be noted that the imaginary frequencies for the transition structures obtained with the two types of calculation are comparable (748i cm^{-1} vs 795i cm^{-1} with the PCM method). Finally, these

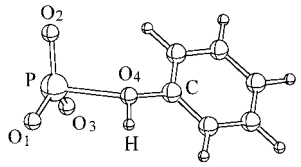

Figure 6. B3LYP-PCM optimized geometry of the zwitterionic form of phenyl phosphate monoanion.

calculations provide an excellent test of the performance of the PCM method for modeling the effect of solvation on the hydrolysis reaction of phosphate monoester monoanions. The present results suggest that the computational approach we have used in the previous paper for modeling the hydrolysis of the methyl phosphate anion is sound and that the solvation effects are properly accounted for.

The calculated free energy values ΔG_{aq} collected in Table 5 make it possible to calculate the pK_a constant for the zwitterionic species $CH_3O^+(H)PO_3^{2-}$ (referred to as pK_Z) from the following thermodynamic cycle:

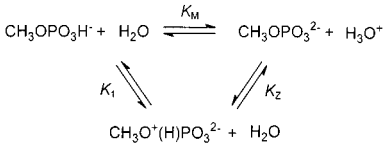

in which K_1 is the equilibrium constant for the prototropic rearrangement investigated ($K_1 = \exp(-\Delta G_{aq}/RT)$), K_M is the experimentally determined acidic constant at 25 °C for methyl phosphate monoanion ($K_M = 10^{-6.58}$),[10] and $K_Z = K_M/K_1$. With a relative free energy value in the range 20.4−20.8 kcal/mol, the computed pK_Z value is on the order of −8.6. Although determined more accurately, this value is not so far from the crude empirical estimation of −4.0 proposed by Kirby and Varvoglis[4] as long ago as 1967. Clearly, such a value allows us to claim that anionic zwitterion **2** cannot be considered as a bimolecular complex of metaphosphate and methanol. Indeed, this species is almost 24 pK_a units more acidic than solvated methanol (pK_a = 15.2).

Substituent Effect on the Geometry of $RO^+(H)PO_3^{2-}$ Species. In this section we examine the effect of ROH (the leaving group for the hydrolysis reaction of $ROPO_3H^-$) on the zwitterionic structures $RO^+(H)PO_3^{2-}$. In our previous paper,[1] anionic zwitterions were identified as intermediates in two cases, R = H and R = CH_3, using PCM geometry optimizations. According to Kirby and Varvoglis,[4] the mechanism of the hydrolysis of $ROPO_3H^-$ depends on the leaving group basicity; the tautomeric form $RO^+(H)PO_3^{2-}$ should intervene as an intermediate only when the leaving group ROH is as basic as phenol (i.e., when p$K_a^{ROH} \geq 10$) but should not play any role as an intermediate when the leaving group basicity falls well below that of phenol (i.e., when p$K_a^{ROH} < 10$; see Scheme 1 and footnote 10 of ref 1). For this reason, we tried to optimize the geometry of the zwitterionic structure $RO^+(H)PO_3^{2-}$ when R = phenyl (p$K_a^{ROH} = 10$) and 2,4-dinitrophenyl (pK_a^{ROH} = 4.07) at the B3LYP-PCM level of theory.

We succeeded for the phenyl phosphate ester for which the fully optimized PCM geometry of the zwitterionic form is represented in Figure 6. Some selected distances are also provided in Table 6. It is very interesting to compare the P−O bond distances between phosphorus and the esterified oxygen for the methyl and phenyl substituents (the P−O_4 distance in Figures 1 and 6). As expected, this distance is markedly larger for the phenyl substituent (by 0.24 Å), indicating a more dissociative character of the zwitterionic species in that case.

TABLE 6: Selected Distances for the Zwitterionic Structure of Phenyl Phosphate Monoanion Optimized with the PCM Solvation Model[a]

$PhO(H)^+PO_3^{2-}$	PCM
P−O_1	1.508
P−O_2	1.506
P−O_3	1.504
P−O_4	2.267
C−O_4	1.397
O_4−H	0.978

[a] Values are calculated using the conventional set of Pauling radii and a dielectric constant of 78.39. All distances are in angstroms. The optimized structure is shown in Figure 6.

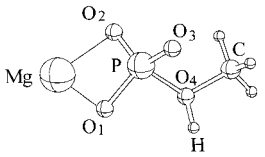

Figure 7. B3LYP optimized geometry of **2** complexed by Mg^{2+} (**2**·Mg^{2+}) in the gas phase.

TABLE 7: Selected Geometrical Parameters for the Fully Optimized 2·Mg^{2+} Structure in the Gas Phase[a]

2·Mg^{2+}	gas
P−O_1	1.570
P−O_2	1.568
P−O_3	1.469
P−O_4	1.898
C−O_4	1.497
O_4−H	0.982
O_1−Mg	1.968
O_2−Mg	1.963
P−O_1−Mg	90.2
O_1−Mg−O_2	76.9
Mg−O_2−P	90.4
O_2−P−O_1	102.2

[a] All distances are in angstroms and angles in degrees. The optimized structure is shown in Figure 7.

In contrast, despite an intensive search on the potential energy surface, a zwitterion-like intermediate could not be located for the 2,4-dinitrophenyl ester at the same level of theory. Any attempt to optimize the zwitterionic form led to the location of the bimolecular complex formed by 2,4-dinitrophenol and the metaphosphate ion. These results as a whole are in perfect agreement with the predictions made by Kirby and Varvoglis 35 years ago based on the observation of a negative deviation of the Brönsted-type linear plot, log k_{hyd} vs pK_a^{ROH}.[4]

Counterion Effect. A zwitterionic intermediate could also be stabilized in the gas phase by taking into account the presence of counterions such as Mg^{2+}. Indeed, a complex between Mg^{2+} and the zwitterionic form **2**, $CH_3O^+(H)PO_3^{2-}$·Mg^{2+}, has been optimized as a minimum on the gas-phase potential energy surface. As shown in Figure 7, the Mg^{2+} ion occupies a bridging position between two oxygen atoms of the metaphosphate fragment. Selected geometrical distances and angles for **2**·Mg^{2+} are listed in Table 7. It can be seen from this table that the P−O bond distance between phosphorus and the esterified oxygen (denoted as P−O_4 in Figure 7) is the shortest we have obtained for anionic zwitterions optimized in this and the previous study.[1]

Bonding Characteristics in 2. To get more electronic information on the nature of the P−O bond between phosphorus and the methyl oxygen, we computed the natural bond orbital (NBO) charges for **2** at the PCM level, and for **2**·$(H_2O)_4$ in the gas phase (Table 8).

TABLE 8: Natural Bond Orbital Populations for 2 (PCM) and 2·$(H_2O)_4$ (Gas Phase)

atom	P	O_1	O_2	O_3	O_4	H	C
2[a]	2.62	−1.26	−1.25	−1.26	−0.82	0.56	−0.19
2·$(H_2O)_4$[b]	2.64	−1.25	−1.20	−1.23	−0.84	0.55	−0.21

[a] Structure shown in Figure 1. [b] Structure shown in Figure 2.

First, we can note that the same charge distribution is obtained using the PCM method or the supermolecule approach. In both cases, phosphorus has a strong positive charge and the esterified oxygen O_4 is negative, conferring a highly polar character to the P−O_4 bond. This can be corroborated by the calculated value of the P−O_4 Wiberg bond index (ca. 0.2), which is much smaller than unity.

Moreover, analysis of the molecular orbitals reveals that the bonding interaction can essentially be described as a donation from the adequate lone pair of the oxygen atom of CH_3OH to the empty orbital of phosphorus perpendicular to the PO_3^- plane. We observed that there is a global charge transfer of 0.15e from methanol to metaphosphate, justifying the name of "anionic zwitterion" given to this species. As expected, this charge transfer is strongly enhanced in a highly polar medium such as water.

Conclusions

According to the results presented in this and our previous paper,[1] anionic zwitterions $RO^+(H)PO_3^{2-}$ can be identified as key intermediates in the dissociative hydrolysis of phosphate monoester monoanions. In the previous paper, we have shown that the PCM solvation model is successful in reproducing the experimental data on the hydrolysis of the methyl phosphate anion **1** provided one explicit water molecule is included in the reactant system. We also found that dielectric effects alone are sufficient to locate the $CH_3O^+(H)PO_3^{2-}$ structure as an intermediate. The present paper shows that the supermolecule approach based on the use of explicit solvent molecules reproduces the PCM results quite closely; both approaches give relative free energies of comparable accuracy. The obvious advantage of the explicit solvation model is that it allows one to gain more information on the number and the position of H_2O molecules necessary to stabilize the zwitterionic species in the absence of a continuum. The present results show that as few as two H_2O molecules are sufficient to locate $CH_3O^+(H)PO_3^{2-}$ as an intermediate provided these specifically solvating water molecules occupy a critical bridging position between the methanol and metaphosphate fragments. Finally, we have also shown that biologically important counterions such as Mg^{2+} could play the same role as water in stabilizing the zwitterionic species $CH_3O^+(H)PO_3^{2-}$ in the gas phase. Work is in progress to determine the extent to which these data can be extrapolated to behavior at an enzyme active site.

Acknowledgment. We thank the Centre Informatique National de l'Enseignement Supérieur (CINES), Montpellier, France, for a generous allocation of computer time (project pqt1073).

References and Notes

(1) Bianciotto, M.; Barthelat, J.-C.; Vigroux, A. *J. Am. Chem. Soc.*, in press.

(2) In the polarizable continuum model PCM the solvent water is treated as a continuous unstructured dielectric with the dielectric constant value of $\epsilon = 78.39$. For details see: Tomasi, J.; Persico, J. *Chem. Rev.* **1994**, *94*, 2027.

(3) Jencks, W. P. *Brookhaven Symp. Biol*. **1962**, *N*° 15, 134.

(4) Kirby, A. J.; Varvoglis, A. G. *J. Am. Chem. Soc.* **1967**, *89*, 415.

(5) Hengge, A. C. In *Comprehensive Biological Catalysis*; Sinnot, M. L., Ed.; Academic Press: London, 1998; Vol. 1, pp 517−542. Benkovic, S. J.; Schray, K. J. In *Transition States of Biochemical Processes*; Gandour, R. D., Schowen, R. L., Eds.; Plenum Press: New York, 1978; pp 493−528. Thatcher, G. R. J.; Kluger, R. *Adv. Phys. Org. Chem.* **1989**, *25*, 99−265.

(6) Read, A. E.; Curtiss, L. A.; Weinhold, F. *Chem. Rev.* **1988**, *88*, 899.

(7) Frisch, M. J.; Trucks, G. W.; Schlegel, H. B.; Scuseria, G. E.; Robb, M. A.; Cheeseman, J. R.; Zakrzewski, V. G.; Montgomery, J. A.; Stratmann, R. E., Jr.; Burant, J. C.; Dapprich, S.; Millam, J. M.; Daniels, A. D.; Kudin, K. N.; Strain, M. C.; Farkas, O.; Tomasi, J.; Barone, V.; Cossi, M.; Cammi, R.; Mennucci, B.; Pomelli, C.; Adamo, C.; Clifford, S.; Ochterski, J.; Petersson, G. A.; Ayala, P. Y.; Cui, Q.; Morokuma, K.; Malick, D. K.; Rabuck, A. D.; Raghavachari, K.; Foresman, J. B.; Cioslowski, J.; Ortiz, J. V.; Baboul, A. G.; Stefanov, B. B.; Liu, G.; Liashenko, A.; Piskorz, P.; Komaromi, I.; Gomperts, R.; Martin, R. L.; Fox, D. J.; Keith, T.; Al-Laham, M. A.; Peng, C. Y.; Nanayakkara, A.; Gonzalez, C.; Challacombe, M.; Gill, P. M. W.; Johnson, B.; Chen, W.; Wong, M. W.; Andres, J. L.; Gonzalez, C.; Head-Gordon, M.; Replogle, E. S.; Pople, J. A. *Gaussian 98*, Revision A.7; Gaussian, Inc.: Pittsburgh, PA, 1998.

(8) Bouteiller, Y.; Mijoule, C.; Nizam, M.; Barthelat, J.-C.; Daudey, J.-P.; Pélissier, M.; Silvi, B. *Mol. Phys.* **1988**, *65*, 295.

(9) Hu, C. H.; Brinck, T. *J. Phys. Chem. A* **1999**, *103*, 5379.

(10) Bunton, C. A.; Llewellyn, D. R.; Oldham, K. G.; Vernon, C. A. *J. Chem. Soc.* **1958**, 3574.